Diamond & Related Materials 76 (2017) 79–85

Contents lists available at ScienceDirect

Diamond & Related Materials

journal homepage: www.elsevier.com/locate/diamond

Effect of surface roughness and H–termination chemistry on diamond's semiconducting surface conductance

T. Wade[a,*], M.W. Geis[a,*], T.H. Fedynyshyn[a], S.A. Vitale[a], J.O. Varghese[a], D.M. Lennon[a], T.A. Grotjohn[b], R.J. Nemanich[c], M.A. Hollis[a]

[a] Lincoln Laboratory, Massachusetts Institute of Technology, Lexington, MA, United States
[b] Electrical and Computer Engineering, Michigan State University, East Lansing, MI, United States
[c] Physics, Arizona State University, Tempe, AZ, United States

ARTICLE INFO

Keywords:
Diamond
Hydrogen-termination
Molecular adsorption
Hole channel

ABSTRACT

The H-terminated surface of diamond when activated with NO_2 produces a surface conduction layer that has been used to make FETs. Variations in processing can significantly affect this conduction layer. This article discusses the effect of diamond surface preparation and H termination procedures on surface conduction. Surface preparations that generate a rough surface result in a more conductive surface with the conductivity increasing with surface roughness. We hypothesize that the increase in conductance with roughness is the result of an increase of reactive sites that generate the carriers. Roughening the diamond surface is just one way to generate these sites and the rough surface is believed to be a separate property from the density of surface reactive sites. The presence of C in the H_2 plasma used for H termination decreases surface conductance. A simple procedure for NO_2 activation is demonstrated. Interpretation of electrical measurements and possible alternatives to activation with NO_2 are discussed. Using Kasu's oxidation model for surface conductance as a guide, compounds other than NO_2 have been found to activate the diamond surface as well.

1. Introduction

The hydrogen-terminated (H-terminated) diamond surface can form a hole conductive layer [1], which has been used to form impressive field effect transistors, FETs. FETs can exhibit current densities > 1 A/mm [2,3], a wide operational temperature range, −263 (10 K) to 400 °C [2], high voltage operation > 1 kV [2,4], and high maximum frequency of oscillation, f_{max}, ~100 GHz [5,6]. Diamond FET's high voltage operation and their inherent high thermal conductivity, ~20 times that of Si, makes these devices superior to those formed in other semiconductors. However, the long-term stability and high resistance of this conductive layer limit diamond's FET applications. While the competing technology, high-frequency high-power AlGaN/GaN FETs, have surface resistance from 300 to 400 $\Omega\,sq^{-1}$ [7], traditional diamond surface FETs have resistance varying from 2500 to 10,000 $\Omega\,sq^{-1}$ [2,3,8]. The mechanism that generates this conductive layer is poorly understood, but empirically the conductivity depends upon the diamond surface preparation procedure, the chemistry used to H terminate the surface, and the chemical treatment and activation after H termination.

This article addresses diamond surface preparation before H termination, and the plasma chemistry during H termination. Empirically we have found that diamonds roughened by etching either in molten $NaNO_3$ or in a H_2-O_2 plasma have a more conductive surface after H termination and activation than smooth polished or epitaxial diamond surfaces. The chemistry of H_2 plasma during H termination affects the conductance of the activated diamond surface. Even small amounts of carbon in the plasma either from residual carbon in the chamber or by addition of CH_4 can increase surface resistance by ~4 times that of carbon-free H-termination plasma. A simple standard activation procedure for NO_2 is demonstrated. The decrease in resistance with a rough surface can be understood using Kasu's model [9,10] of partial oxidation of the diamond surface by NO_2. Using this model as a guide other chemistries have been demonstrated to activate diamond at the same level as NO_2.

To be complete, there are other activation chemistries using Al_2O_3 [2,3], SiO_2 [11] and transition metal oxides, primarily MoO_3 and V_2O_5 [12–15]. They have surface resistances from 2.5 to 10 $k\Omega\,sq^{-1}$, while NO_2 activation generates surface resistances from 1 to 2 $k\Omega\,sq^{-1}$. However, NO_2 activation is unstable with the resistance increasing to > 3 $k\Omega\,sq^{-1}$ within a few hours in laboratory air. As the lowest reported resistance surface chemistry known to date, we primarily

* Corresponding authors.
E-mail addresses: Travis.Wade@LL.mit.edu (T. Wade), Geis@LL.mit.edu (M.W. Geis).

http://dx.doi.org/10.1016/j.diamond.2017.04.012
Received 21 March 2017; Received in revised form 9 April 2017; Accepted 10 April 2017
Available online 22 April 2017
0925-9635/

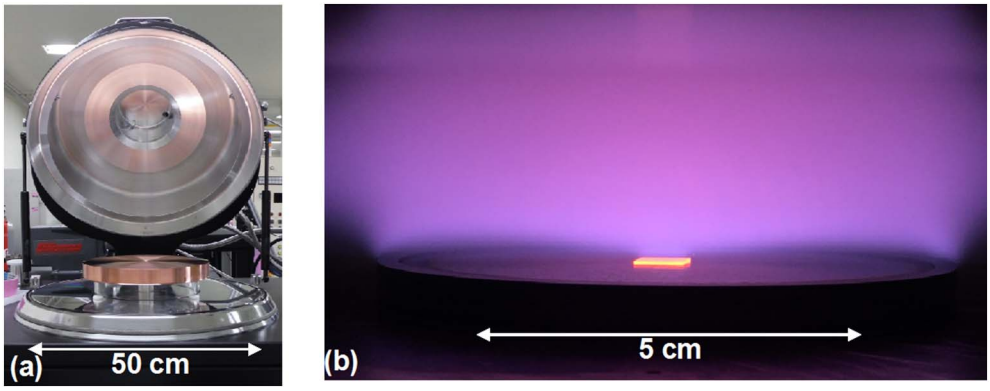

Fig. 1. Diamond growth and H-termination system. (a) Photograph supplied by Seki Diamond Systems of the system, aluminum chamber with a microwave-driven water-cooled copper table. (b) Photograph of 7 × 7 mm diamond during H termination, glowing orange at ~750 °C. The diamond is placed on a Mo plate 7.5 cm in diameter on the copper table shown in Fig. 1a.

consider NO_2 activation in this article.

2. Experimental procedure and characterization

Optical grade, (100)-oriented polished diamonds were obtained from a commercial source and were either 7 × 7 mm or 4.5 × 4.5 mm, 0.5 mm thick and polished to better than 5 nm RMS roughness. The diamonds were cleaned, unless otherwise noted, in molten $NaNO_3$ between 500 and 560 °C for 5 min and then allowed to cool to room temperature before the diamonds were removed by dissolving the $NaNO_3$ in warm water. They were placed in a mixture of 1:1 H_2SO_4 and H_2O_2 and heated from room temperature to 300 °C, rinsed in water followed by acetone and finally ashed in He + 3% O_2 plasma for 5 min. This resulted in a slightly rougher surface than the initial polished diamonds. Diamond cleaned in $NaNO_3$ consistently exhibited higher surface conductance than diamonds cleaned without the $NaNO_3$ step.

H termination was accomplished in a microwave plasma system shown in Fig. 1. The hydrogen pressure, microwave power, and diamond temperature as a function of time during H termination are shown in Fig. 2. For some experiments CH_4 or O_2 was added during H termination.

After H termination the diamond was mounted on a Van der Pauw-Hall probe, Fig. 3, and activated for 1 min in an atmosphere of nitrogen dioxide, NO_2. The NO_2 was generated by placing copper foil cuttings in concentrated, 70% nitric acid. Either a flat bottomed glass evaporation dish with a cover glass or a sealable plastic bag is used as a container. The heaver NO_2 displaces the air in the container. The plastic bag is used when Hall measurements in NO_2 are required. After H termination the diamond was usually activated within a few minutes to minimize air contamination. However, we have observed no conduction difference when several hours in laboratory air separated H termination and activation. Fig. 4 shows one frame of the supplemental movie of the procedure. Surface resistance was observed to saturate within seconds after exposure to NO_2. After activation the diamond, still mounted on

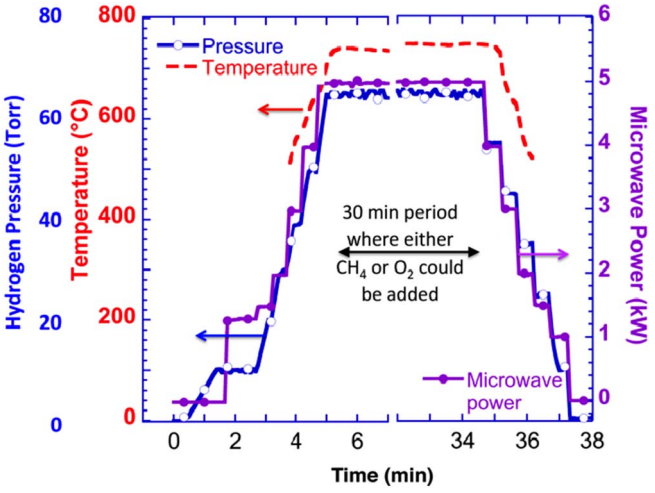

Fig. 2. H_2 pressure, diamond temperature, and 2.54 GHz microwave power as a function of time during H termination. The H_2 pressure and the microwave power were gradually increased over a 3-minute period to 65 Torr (8.7 kPa) and 5 kW, which was maintained for a 30-minute period. Either CH_4 or O_2 could be added to the chamber during this period. The power and pressure were then gradually decreased. A two-color, 2.1 and 2.4 μm, optical pyrometer measured the temperature. These optical wavelengths may not be the best for accurate temperature measurements.

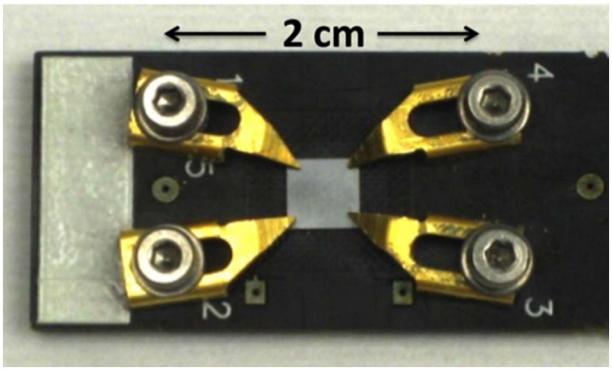

Fig. 3. Photograph of a 4.5 × 4.5 mm diamond mounted for resistance and Hall measurements. Gold plated clips form the corners of a 3.1 mm square. During H termination and activation the back and edges of the diamond become conductive to a lesser degree than the front surface. To avoid compromising the measurements the back and edges of some diamonds were rubbed with 1-μm Al_2O_3 abrasive powder, which makes the surface insulating. This procedure did not appreciably change the electrical measurements and was discontinued. (For interpretation of the references to color in this figure legend, the reader is referred to the web version of this article.)

Fig. 4. NO_2 activation of H-terminated diamond. The NO_2 is generated by the chemical reaction, $4HNO_3 + Cu \rightarrow Cu(NO_3)_2 + 2NO_2 + 2H_2O$. The supplemental movie shows the activation procedure. A small plastic bag filled with NO_2 is used instead of a glass container when Hall measurements are required.

the probe, is placed in flowing dry N_2. The surface resistance, carrier density, and carrier mobility were measured with a 0.75 T permanent magnet during NO_2 activation and a 2 T electromagnet when in flowing N_2. As expected, mobility measurements did not vary when the magnetic field was varied between 0.1 and 2 T, since the Hall mobility times the magnetic field for these experiments is always $< 2 \times 10^{-2}$ [16], which insures that the magnetic field does not significantly alter the current flow in the Van der Pauw structure.

3. Diamond surface preparation

We have observed that diamonds with surfaces roughened with molten $NaNO_3$ were more conductive than similar polished diamonds. To better characterize this observation, a series of experiments were performed to progressively roughen a polished diamond. A 7 × 7 mm diamond cleaned without molten $NaNO_3$ was H-terminated, activated and had roughness measured using a Zygo Nexview optical surface profiler. It was then plasma etched at 65 Torr (8.7 kPa) of H_2 + 4% O_2 plasma with 5.5 kW microwave power to roughen the surface, after which it was cleaned without $NaNO_3$, H terminated, activated, and re-characterized. The procedure was repeated until the RMS roughness was ~0.5 μm and the electrical properties did not change with additional etching. The RMS roughness as a function of etch time is shown by the inset of Fig. 6. Fig. 5 is a photograph of two 7 × 7 mm diamonds, on the left is a polished diamond and on the right a diamond after 175 min of etching resulting in 450 nm RMS roughness.

As shown in Fig. 6, after each etching the resistance of the diamond decreased. Fig. 7 shows the diamond surface after 175 min of etching, 450 nm RMS roughness, with a surface resistance < 2-kΩ sq.$^{-1}$. The mobility decreased with increasing roughness, but this was more than compensated by the increase in carrier density as shown in Figs. 8 and 9. With regards to extremely low roughnesses, 0.4 nm Ra, CMP polished surfaces produced results indistinguishable from 5 nm Ra scaif-polished surfaces.

Scanning electron micrograph, SEM, Fig. 7 shows the diamond roughness is a series of pits with their sides consisting of steps. One surface is nearly parallel to the (100) surface of the diamond and the other slopes downward. Atomic force microscopy, AFM, Figs. 10 and 11, across the etch pit is instructive. The pits are inverted pyramids with different sidewall angles from normal and at different etched depths, perhaps depending upon the crystal defect responsible for the pit formation. A higher resolution AFM image of one step, Figs. 12 and 13, show the downward sloped facet to be ~44° from normal. The AFM uses a tip with a 2 nm radius and its forward and rear angles are 15 and 25° respectively [17]. The tip angles are smaller than the measured angle of the pit's wall, minimizing image artifacts. Similar etch pits with stepped sidewalls were observed on steam etched diamond at 800 °C [18].

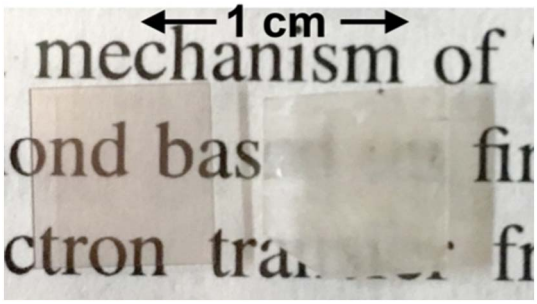

Fig. 5. Optical image of two diamonds. On the left is a polished 7 × 7 mm diamond. The letters can be easily visualized through the diamond. On the right is the 450 nm RMS roughened diamond used in this experiment. The letters are barely discernible through the frosted diamond surface.

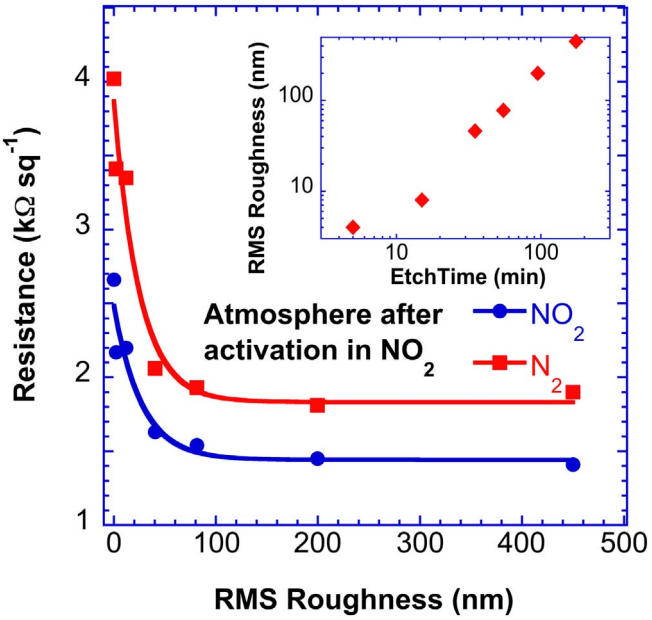

Fig. 6. Resistance of a (100)-oriented diamond as a function of surface roughness. The blue curve, circular data points, is the resistance while in NO_2 after ~1 min of activation and the red curve, square data points, is the same diamond when NO_2 is followed with dry N_2. The curves are an aid to eye. The inset shows the RMS roughness as a function of etching time. (For interpretation of the references to color in this figure legend, the reader is referred to the web version of this article.)

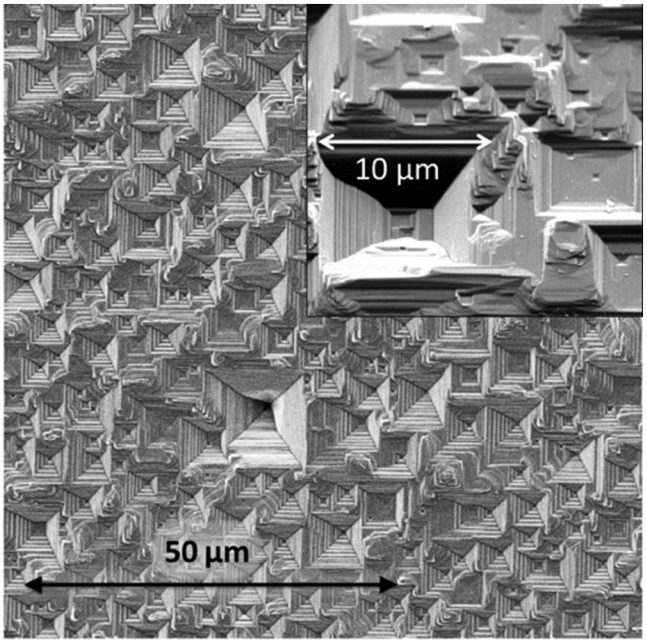

Fig. 7. Scanning electron micrograph, SEM, of the diamond surface after 175 min of etching in a plasma of 4% O_2 in H_2. The surface consists of pits with sidewalls formed by horizontal planes approximately parallel to the (100) diamond surface and more vertical planes ~44° to the substrate normal. RMS roughness is ~450 nm. Inset is a higher magnification showing the stepped surface.

4. Effect of H-termination chemistry

The H-termination system is also used to grow epitaxial diamond using CH_4, which results in high levels of residual carbon contamination in the system. When the system was cleaned of carbon by running with 4% O_2 in H_2 for an hour prior to H-termination, higher surface conductivity is observed compared to diamonds which are H-terminated in the carbon-contaminated system. To better understand this,

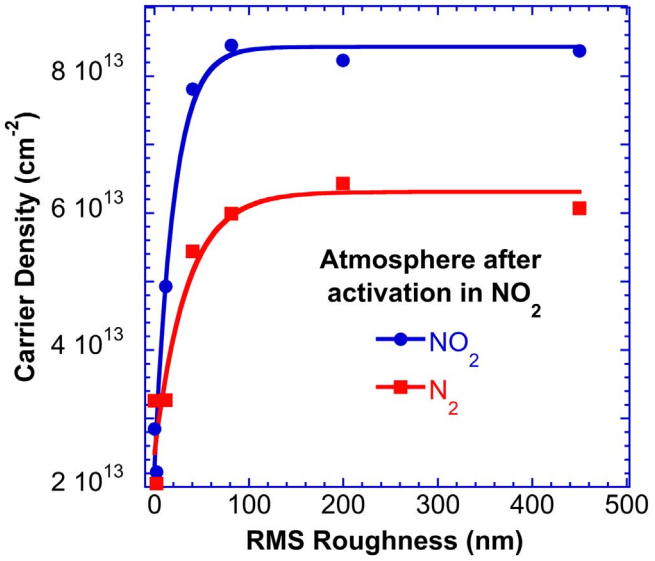

Fig. 8. Carrier density of a (100)-oriented diamond as a function of surface roughness. The blue curve, circular data points, is the carrier density while in NO_2 and the red curve, square data points, is the same diamond when NO_2 is replaced with dry N_2. The curves are an aid to eye. (For interpretation of the references to color in this figure legend, the reader is referred to the web version of this article.)

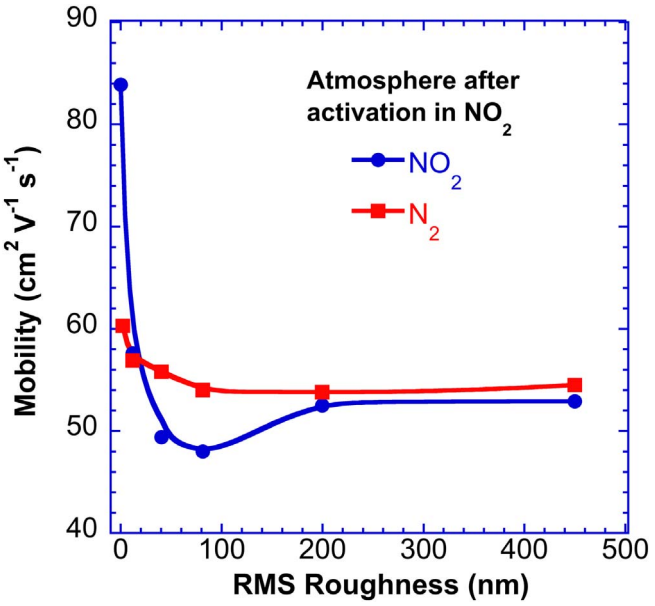

Fig. 9. Hall carrier mobility of a (100)-oriented diamond as a function of surface roughness. The blue curve, circular data points, is the mobility while in NO_2 and the red curve, square data points, is the same diamond when NO_2 is replaced with dry N_2. The curves are an aid to eye. (For interpretation of the references to color in this figure legend, the reader is referred to the web version of this article.)

four 4.5 × 4.5-mm diamonds were selected that exhibited H-termination activation conductance ratios between the diamonds < 1.5. Each of the diamonds was H-terminated in a different atmosphere, H_2 with 0.2% CH_4, H_2, H_2 with 0.5% O_2 and H_2 with 10% O_2. After H termination they were activated in NO_2 and electrically characterized in NO_2 and then in dry flowing N_2. The results are shown in Figs. 14–16.

The best results were obtained with just H_2 with some reduction in conductivity with the addition of O_2, but a significant reduction in conductivity occurred with the addition of even a small percentage of CH_4.

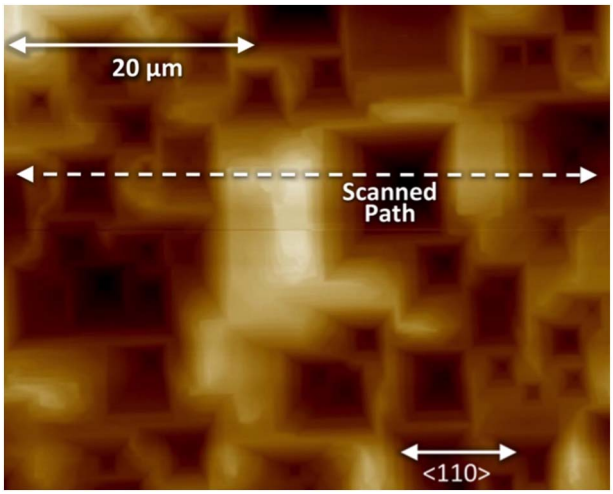

Fig. 10. Atomic force microscope, AFM, image of a portion of the etched diamond shown in Fig. 7.

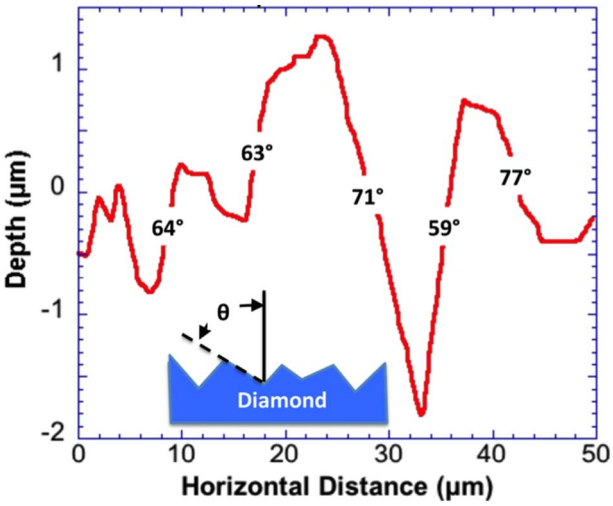

Fig. 11. An AFM depth profile across the dashed line shown in Fig. 10.

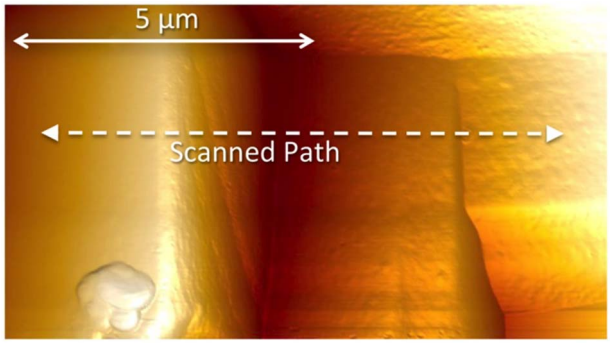

Fig. 12. AFM of the sidewall of a etch pit showing the surface steps in Figs. 7 and 10 at a higher magnification. The dotted line represents the path shown in Fig. 13.

5. Discussion

5.1. Corrections for electrical measurements

Other than actually characterizing diamond FETs, the majority of the electrical characterization is performed with Van der Pauw probes and Hall mobility measurements, an example is shown in Fig. 3. These measurements are used to determine the surface conductance and the carrier drift mobility. To obtain these properties from Van der Pauw

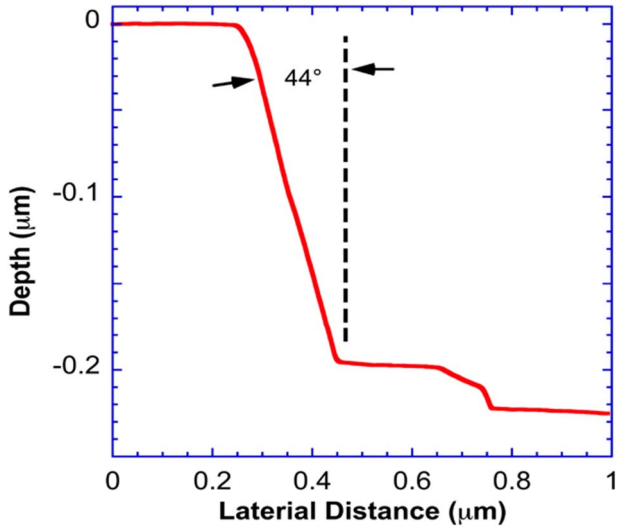

Fig. 13. Depth profile of the dashed line in Fig. 12. The sidewall makes an angle of ~44° with the normal to the horizontal step.

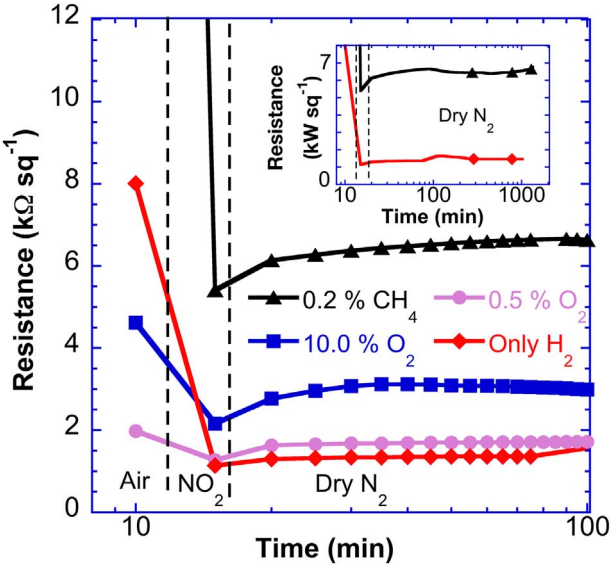

Fig. 14. Resistance for various H-termination conditions with various gases added to an otherwise pure hydrogen plasma. The measurements were made in air, in NO_2, and in flowing dry N_2. The air measurements varied with the time required to mount the sample, but this variation does not affect NO_2 or N_2 measurements. In dry N_2 the resistance varies < ± 10% over 16 h as shown by the inset. On subsequent H-termination with only H_2, the diamond pitted in the 10% O_2-H_2 plasma had the highest conductance of this group of four diamonds. These 4.5 × 4.5 mm diamonds were more conductive than the 7 × 7 mm diamond previously discussed. Diamonds from different suppliers commonly gave very different conductance.

resistive and Hall voltage measurements, corrections for the geometric placement of electrodes on the diamond surface and the fundamental ratio of the Hall and drift mobilities should be considered.

Because the probes are not at the edges of the diamond to make an ideal Van der Pauw measurement and the sides of the substrate may be conductive, the measured Van der Pauw resistance will be less than the actual resistance and the measured Hall mobility will be less than the actual value. Assuming only the top surface of the 4.5 × 4.5 mm diamond is conductive and the probes form a 3.1 × 3.1 mm square, as in Fig. 3, then the measured surface resistance measurement will be 3.5% below the actual value [19]. The measured Hall mobility will be 13% lower than the actual value [20]. Small variations from the ideal Van der Pauw structure require only small second order corrections for resistance measurements, but higher than first order corrections are required for mobility measurements [16,21].

A separate correction is required to obtain the drift mobility from the Hall mobility. The Hall coefficient factor, the ratio of the Hall and drift mobilities, is a fundamental property of the semiconductor and for bulk diamond it is 0.6 to 0.7 [22]. However, the ratio for a surface conductive layer with a reconstructed diamond surface is unknown and may be different for different crystal planes. Considering a geometric correction factor of 13% and assuming a Hall factor of 0.6 then the drift mobility is approximately twice that of the measured value and the carrier density is half of its calculated value. Due to the uncertainty in these correction factors as they apply to diamond, no corrections for geometry or Hall factor have been made for data in this paper. As a result, resistance measurements can be accepted to be accurate within ~3.5%, but carrier density and mobility are likely to deviate significant from the actual value.

5.2. Electrical properties

Rough surfaced diamond substrates have a higher conductivity than smooth polished diamond surfaces. Polished diamond abraded with diamond grit exhibits a ~20% increase in conductance and diamonds that have their entire surface roughened with diamond grit on a polishing wheel have conductance similar to the plasma-etched diamonds of Fig. 6. From the depth profile and angles of the etched diamond shown in Fig. 11, the calculated increase in surface area over a smooth surface is only < 20%. This surface area increase is insufficient to explain the increase in carrier density by 3.9 in NO_2 and 3 in N_2 between smooth and rough surfaces.

The hole surface carriers observed to date have Hall mobilities from 30 to 200 $cm^2 V^{-1} s^{-1}$. Assuming that the drift mobilities differ from Hall mobilities by less than a factor of two, then the maximum drift mobility is < 400 $cm^2 V^{-1} s^{-1}$. This is considerably less than diamond's highest-reported hole drift mobility of 3800 $cm^2 V^{-1} s^{-1}$ at room-temperature [23]. Kasu et al. [10] suggested that the reduced mobility is the result of islands of conductance separated by regions of poorer conductance resulting in reduced mobility when the sample is large compared to the size of the islands. Another possibility is the electric field normal to the diamond surface between the negative charge on the surface and the positive holes in the diamond will pull the holes to the surface of the diamond where surface roughness increases carrier scattering and reduces mobility. This scattering model is consistent with the observation that when the carrier density increases as the electric field normal the surface increases then the mobility decreases. Similar effects have been observed in silicon [24,25]. Our optical profilometry surface roughness measurements can only characterize surface variations > 100 nm in width. Assuming a mean hole mobility of 100 $cm^2 V^{-1} s^{-1}$, effective mass of 0.7 m_h and a thermal velocity of 10^7 cm s^{-1} the mean fee path of carriers in the diamond is ~4 nm. Therefore, our surface roughness measurements do not directly indicate whether surface roughness affects the hole mobility, leaving the cause of reduced mobility still unknown.

For 20 years, without any physical evidence, it was widely believed that NO_2 formed NO_2^- on the surface of the diamond by removing a valence electron from the diamond, creating a hole surface conductive layer in the diamond (charge transfer doping) [26,27]. However in 2010 Kasu et al. [9,10] probed the surface using X-ray photoelectron spectroscopy, XPS, and found that diamond activated by NO_2 had no surface nitrogen. He speculated that two mechanisms were responsible for NO_2 activation. First of these is a charge transfer doping mechanism where NO_2 forms a negative ion on the diamond surface, which generates a conductive hole in the diamond. The second mechanism where the NO_2 chemically reacts with the diamond surface and departs leaving behind a molecular structure composed of O, C, and H atoms which also form a negative ion. These two mechanisms are schematically shown in Fig. 17. Our Attenuation-Transmission–Reflection Fourier-Transform-Infrared (ATR-FTIR) observations on single-crystal

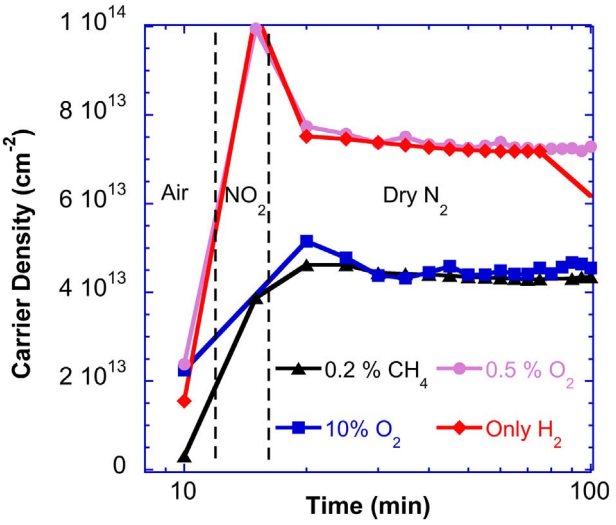

Fig. 15. Carrier density for several gaseous conditions during H termination.

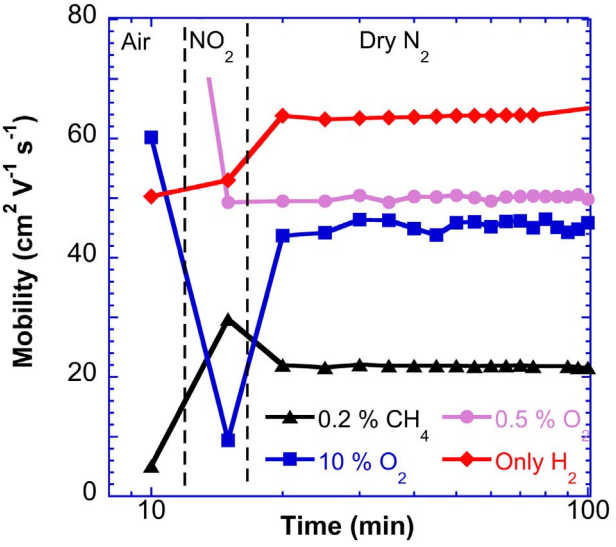

Fig. 16. Hall carrier mobility for several gaseous conditions during H termination.

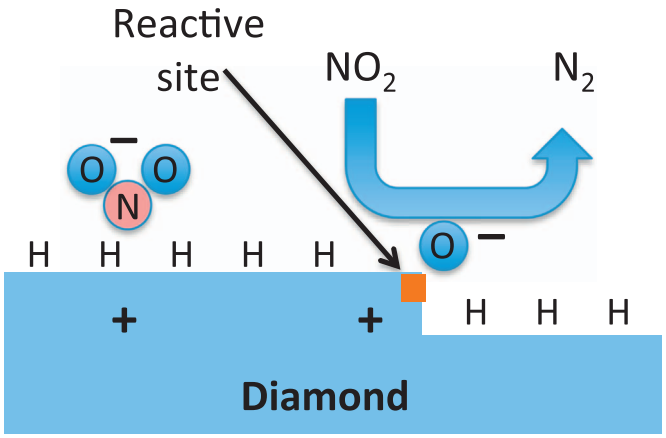

Fig. 17. Conceptual drawing showing a negative NO_2 ion as a charge transfer mechanism to generate a positive hole (left). An alternative model is discussed by Kasu [10] where holes are generated by a negative ion C, H, and O complex formed during a chemical reaction between NO_2 and the diamond surface (right).

H-terminated NO_2-activated diamond exhibit no optical absorption for NO_2, N_2O_4 or NO_2^-. We speculate that NO_2 reacts at sites where the diamond surface terrace is disrupted, such as atomic surface steps [28,29] and kinks, at double or triple carbon-carbon bonds, or at radical sites. This theory represents a deviation from the widely-held model for transfer doping involving an idealized diamond surface. Further proof and development of this theory will involve deliberate surface engineering and creates the potential for directionally asymmetric surface conduction.

Assuming the average number of atoms on the surface is the (atomic density)$^{2/3}$, $(1.77 \times 10^{23})^{2/3}$ or 3.2×10^{15} cm^{-2}, and the highest carrier density calculated from the Hall mobility is $\sim 10^{14}$ cm^{-2}, if corrected for geometric and Hall coefficient factors, the carrier density is $\sim 5 \times 10^{13}$ cm^{-2} A large fraction of the surface, 1.6%, would have to have reactive sites. We speculate that roughening the diamond surface is one method of increasing these sites while H terminating with CH_4 in the H_2 plasma decreases these sites.

Looking for alternative methods of activation other than NO_2 and using Kasu's oxidation concept we have found other compounds that have selective and limited oxidation properties, such as $(NH_4)_3Ce(NO_3)_6$ [30,31] in an aqueous acid solution and photo-generated radicals in an oxygen atmosphere (UV-activated Irgacure 819 [32]). These materials activate the surface of diamond at a similar level as that obtained with NO_2. More aggressive oxidizing solutions, such as $(NH_4)_3Ce(NO_3)_6$ in acetic acid [30], result in an insulating surface.

Other researchers [31] have reported that an NO_2 activated diamond exhibits a significant decrease in carrier density (a factor of 3) with a corresponding increase in resistance over the first few hours even in high purity N_2. As reported here using humid NO_2 at higher concentrations for activation, carrier densities and resistance in dry N_2 varied by $< \pm 10\%$ over 16 h, as shown by the inset in Fig. 14. Fig. 18 shows a ~40% resistance increase in 120 h. In contrast, in laboratory air the carrier density decreases by 60 to 70% over a few hours. The cause of this variation in carrier stability is unknown.

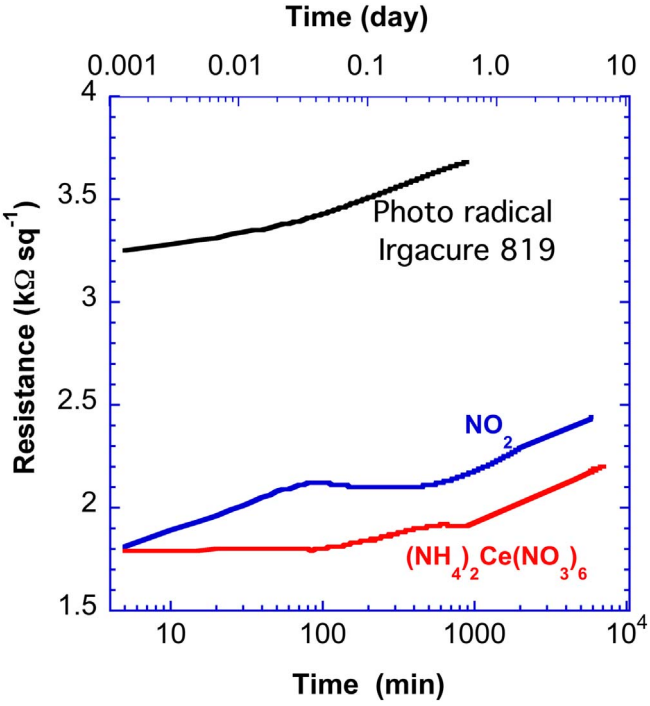

Fig. 18. The resistivity of three activated chemistries diamonds in N_2 over time. Irgacure 819 activation was obtained by depositing a thin film of it from a CCl_4 solution on a diamond and exposing it in air or O_2 to 365 nm light, 0.7 mW cm^{-2}, until the resistance stabilized, ~5 min. $(NH_4)_3Ce(NO_3)_6$ activated by soaking the diamond in H_2O solution of $(NH_4)_3Ce(NO_3)_6$ with HNO_3 or $HClO_4$. The diamond is blown dry in flowing N_2 without a water rinse.

6. Summary

In summary we have demonstrated that roughening the diamond surface increases surface conductance by increasing carrier density by 3–4 times while incurring a relatively small decrease in carrier mobility. The increase in conductance is believed not to be a function of roughness, but the result of an increase in reactive sites enhancing the carrier density. Roughening the diamond surface is just one way to generate these sites and the rough surface is believed to be a separate property from the density of surface reactive sites. An alternative model is that etching the diamond to roughen it removes surface damage that limits the conductivity. However, this seems unlikely as physically abrading the diamond surface with diamond grit also decreases resistance.

Carbon in the H-plasma during H termination reduces diamond's surface conductance, which we speculated reduces these reactive sites. A simple standard NO_2 activation procedure was demonstrated and the possibility of other activation compounds and procedures using a model of activation by limited oxidation was discussed. Diamond surfaces H terminated, activated, and placed in dry N_2 demonstrate stable electrical properties over several days, while others have found the carrier densities decreased by several-fold over the same period even in high purity N_2 [33]. The results reported here are primarily for activation with NO_2. Other activation chemistries with MoO_3, V_2O_5, [12–15] and $(NH_4)_3Ce(NO_3)_6$ may not have the same conductance variation with surface roughness or H-termination chemistries as NO_2. The chemistry of charge transfer doping mechanism with NO_2 appears to differ from the doping mechanism with MoO_3 and V_2O_5 [12–15]. Additional research will clarify the difference.

Acknowledgement

The authors are grateful for the expert technical assistance of Michael Marchant and Peter Murphy. DISTRIBUTION STATEMENT A: Approved for public release: distribution unlimited. This material is based upon work supported by the Assistant Secretary of Defense for Research and Engineering under Air Force Contract No. FA8721-05-C-0002 and/or FA8702-15-D-0001. Any opinions, findings, conclusions or recommendations expressed in this material are those of the author(s) and do not necessarily reflect the views of the Assistant Secretary of Defense for Research and Engineering.

Appendix A. Supplementary data

The Supplemental movie associated with this article can be found here. http://dx.doi.org/10.1016/j.diamond.2017.04.012.

References

[1] M.I. Landstrass, K.V. Ravi, Resistivity of chemical vapor deposited diamond films, Appl. Phys. Lett. 55 (1989) 975–977.
[2] H. Kawarada, T. Yamada, D. Xu, H. Tsuboi, T. Saito, A. Hiraiwa, Wide temperature (10K–700K) and high voltage (~1000V) operation of C−H diamond MOSFETs for power electronics application, Electron Device Meeting (IEDM), IEEE Int. 11 (2) (2014) 1–4, http://dx.doi.org/10.1109/IEDM.2014.7047030.
[3] K. Hirama, H. Sato, Y. Harada, H. Yamamoto, M. Kasu, Diamond field-effect transistors with 1.3 A/mm drain current density by Al_2O_3 passivation layer, Jpn. J. Appl. Phys. 51 (2012) 090112.
[4] M. Syamsul, Y. Kitabayashi, D. Matsumura, T. Saito, Y. Shintani, H. Kawarada, High voltage breakdown (1.8 kV) of hydrogenated black diamond field effect transistor, Appl. Phys. Lett. 109 (2016) 203504.
[5] D.A.J. Moran, S.A.O. Russell, S. Sharabi, A. Tallaire, High frequency Hydrogen-terminated diamond field effect transistor technology, 12th IEEE International Conference on Nanotechnology (IEEE-NANO) 20–23 August 2012, Birmingham, United Kingdom, 2012.
[6] M. Kasu, Diamond field-effect transistors for RF power electronics: novel NO_2 hole doping and low temperature deposited Al2O3 passivation, Jpn. J. Appl. Phys. 56 (2017) 01AA01.
[7] J. Lehmann, C. Leroux, M. Charles, A. Torres, E. Morvan, D. Blachier, G. Ghibaudo, E. Bano, G. Reimbold, Sheet resistance measurement on AlGaN/GaN wafers and dispersion study, Microelectron. Eng. 109 (2013) 334–337.
[8] C. Verona, W. Ciccognani, S. Colangeli, E. Limiti, M. Marinelli, G. Verona-Rinati, D. Cannatà, M. Benetti, F. Di Pietranton, V_2O_5 MISFETs on H-terminated diamond, IEEE Trans. Electron Devices 63 (2016) 4647–4653.
[9] M. Kubovic, M. Kasu, H. Kageshima, F. Maeda, Electronic and surface properties of H-terminated diamond surface affected by NO_2 gas, Diam. Relat. Mater. 19 (2010) 889–893.
[10] H. Sato, M. Kasu, Electronic properties of H-terminated diamond during NO_2 and O_3 adsorption and desorption, Diam. Relat. Mater. 24 (2012) 99–103;
M. Kasu, H. Sato, M. Kubovic, Hole Carrier Doping on NO_2 and O_3 adsorption on H-terminated diamond surface, in special issue: unusual surface science of carbon-based materials, Surf. Sci. 33 (2012) 575–582 ((in Japanese) see: NO2 およびO3 吸着による水素終端ダイヤモンド表面の 正孔ドーピング).
[11] M.J. Sear, A.K. Schenk, A. Tadich, A. Stacey, C.I. Pake, P-type surface transfer doping of oxidized silicon terminated (100) diamond, Appl. Phys. Lett. 110 (2017) 011605.
[12] S.A.O. Russell, L. Cao, D. Qi, A. Tallaire, K.G. Crawford, A.T.S. Wee, D.A.J. Moran, Surface transfer doping of diamond by MoO_3: a combined spectroscopic and Hall measurement study, Appl. Phys. Lett. 103 (2013) 202112.
[13] M. Tordjman, C. Saguy, A. Bolker, R. Kalish, Superior surface transfer doping of diamond with MoO_3, Adv. Mater. Interfaces 1 (1) (2014) 1300155, http://dx.doi.org/10.1002/admi.201300155.
[14] K.G. Crawford, L. Cao, D. Qi, A. Tallaire, E. Limiti, C. Verona, A.T.S. Wee, D.A.J. Moran, Enhanced surface transfer doping of diamond by V_2O_5 with improved thermal stability, Appl. Phys. Lett. 108 (2016) 042103.
[15] C. Verona, W. Ciccognani, S. Colangeli, E. Limiti, Marco Marinelli, G. Verona-Rinati, Comparative investigation of surface transfer doping of hydrogen terminated diamond by high electron affinity insulators, J. Appl. Phys. 120 (2016) 025104.
[16] I. Miccoli, F. Edler, H. Pfnur, C. Tegenkamp, The 100th anniversary of the four-point probe technique: the role of probe geometries in isotropic and anisotropic systems, J. Phys. Condens. Matter 27 (2015) 223201, http://dx.doi.org/10.1088/0953-8984/27/22/223201.
[17] http://www.brukerafmprobes.com/Product.aspx?ProductID=3726.
[18] J. Zhang, T. Nakai, M. Uno, Y. Nishiki, W. Sugimoto, Preferential {100} etching of boron-doped diamond electrodes and diamond particles by CO_2 activation, Carbon 70 (2014) 207–214.
[19] A. Mircea, Semiconductor sheet resistivity measurements on square samples, J. Sci. Instrum. 14 (1964) 679–681.
[20] J.D. Weiss, Electrostatics analysis of two Hall measurement configurations, Solid State Electron. 75 (2012) 37–42.
[21] L.J. van der Pauw, A method of measuring specific resistance and Hall effect of discs of arbitrary shape, Philips Tech. Rep. 13 (1958) 1–9.
[22] L. Reggiani, D. Waechter, S. Zukotynski, Hall-coefficient factor and inverse valence-band parameters of holes in natural diamond, Phys. Rev. B 28 (1983) 3550–3554.
[23] J. Isberg, J. Hammersberg, E. Johansson, T. Wikstrom, D.J. Twitchen, A.J. Whitehead, S.E. Coe, G.A. Scarsbrook, High carrier mobility single-crystal plasma-deposited diamond, Science 297 (2002) 1670–1672.
[24] S.C. Sun, J.D. Plummer, Electron mobility in inversion and accumulation layers on thermally oxidized silicon surfaces, IEEE Trans. Electron Dev. 21 (1980) 1497–1508.
[25] S. Yamakawa, H. Ueno, K. Taniguchi, C. Hamaguchi, K. Miyatsuji, K. Masaki, U. Ravaioli, Study of interface roughness dependence of electron mobility in Si inversion layers using the Monte Carlo method, J. Appl. Phys. 79 (1996) 911–916.
[26] R.G. Gi, T. Ishikawa, S. Tanaka, T. Kimura, Y. Akiba, M. Iida, Possibility of realizing a gas sensor using surface conductive layer on diamond films, Jpn. J. Appl. Phys. 36 (1997) 2057–2060.
[27] P. Rivero, W. Shelton, V. Meunier, Surface properties of hydrogenated diamond in the presence of adsorbents: a hybrid functional DFT study, Carbon 110 (2016) 469–479.
[28] M. Geis, T. Wade, T. Fedynyshyn, S. Vitale, T. Grotjohn, R. Nemanich, M. Hollis, Comparison of High-Frequency, High-Power Diamond-Transistor Performance to Other Semiconductor Systems, Fall MRS Conference, (2016) (Boston).
[29] T. Wade, M. Geis, T. Fedynyshyn, S. Vitale, T. Grotjohn, R. Nemanich, M. Hollis, Controlling the Stability of Diamond's Surface Conductivity, Fall MRS Conference, (2016) (Boston).
[30] W.S. Trahanov, L.B. Young, Controlled oxidation of organic compounds with Cerium(IV). 11. The oxidation of toluenes, J. Organomet. Chem. 31 (1966) 2033–2035.
[31] Tse-Lok Ho, Cerium(IV) Oxidation of Organic Compounds, ch11, in: W.J. Mijs, C.R.H.I. de Jonge (Eds.), Organic Syntheses by Oxidation with Metal Compounds, Springer, US, 1986.
[32] Ciba® IRGACURE® 819 Photoinitiator, www.xtgchem.cn/upload/20110629045602.PDF.
[33] M. Kubovic, M. Kasu, Enhancement and stabilization of hole concentration of hydrogen-terminated diamond surface using ozone adsorbates, Jpn. J. Appl. Phys. 49 (2010) 110208.